BBA - Proteins and Proteomics 1869 (2021) 140662

Contents lists available at ScienceDirect

BBA - Proteins and Proteomics

journal homepage: www.elsevier.com/locate/bbapap

Research Paper

Probing the role of Val228 on the catalytic activity of *Scytalidium* catalase

Gunce Goc [a], Sinem Balci [a], Briony A. Yorke [b], Arwen R. Pearson [c], Yonca Yuzugullu Karakus [a,*]

[a] Department of Biology, Kocaeli University, Umuttepe, Kocaeli 41380, Turkey
[b] School of Chemistry and Bioscience, Faculty of Life Sciences, University of Bradford, Bradford West Yorkshire BD7 1DP, UK
[c] The Hamburg Centre for Ultrafast Imaging, Institute for Nanostructure and Solid State Physics, Universität Hamburg, Hamburg, 22761, Germany

ARTICLE INFO

Keywords:
Catalase
Oxidase
Lateral channel
Heme
Catechol

ABSTRACT

Scytalidium catalase is a homotetramer including heme *d* in each subunit. Its primary function is the dismutation of H_2O_2 to water and oxygen, but it is also able to oxidase various small organic compounds including catechol and phenol. The crystal structure of *Scytalidium* catalase reveals the presence of three linked channels providing access to the exterior like other catalases reported so far. The function of these channels has been extensively studied, revealing the possible routes for substrate flow and product release. In this report, we have focussed on the semi-conserved residue Val228, located near to the vinyl groups of the heme at the opening of the lateral channel. Its replacement with Ala, Ser, Gly, Cys, Phe and Ile were tested. We observed a significant decrease in catalytic efficiency in all mutants with the exception of a remarkable increase in oxidase activity when Val228 was mutated to either Ala, Gly or Ser. The reduced catalytic efficiencies are characterized in terms of the restriction of hydrogen peroxide as electron acceptor in the active centre resulting from the opening of lateral channel inlet by introducing the smaller side chain residues. On the other hand, the increased oxidase activity is explained by allowing the suitable electron donor to approach more closely to the heme. The crystal structures of V228C and V228I were determined at 1.41 and 1.47 Å resolution, respectively. The lateral channels of the V228C and V228I presented a broadly identical chain of arranged waters to that observed for wild-type enzyme.

1. Introduction

Catalases (EC 1.11.1.6, Pfam domain ID PF00199) are metalloenzymes found in almost all aerobic organisms [17,26]. They catalyze the degradation of hydrogen peroxide to water and dioxygen. Catalases have been divided into three groups: monofunctional heme (typical) catalases, catalase-peroxidases, and non heme manganese catalases. The monofunctional catalases constitute the largest and most extensively studied group of catalases. They can be subdivided depending on the structure of prosthetic heme group. Small subunit (55–69 kDa) catalases are shown to possess *b* type heme (a pentacoordinated iron protoporphyrin IX), whereas large subunit catalases (75–84 kDa) contain *d* type heme, which is the 180-degree rotated and oxidized form of heme *b* [23]. The change of heme *b* to heme *d* has been investigated in Hydroperoxidase II (HPII) enzyme and suggested to be catalyzed by HPII itself when peroxide or singlet oxygen is present [4,8,22].

Most of monofunctional (typical) catalases extensively studied in detail have all been confirmed to be active as tetramers, even though dimeric, hexameric enzymes have been reported but never conclusively characterized [29]. Over than 250 known sequences of monofunctional type catalases are accessible with the evolutionary relationships discussed respectively [12,18–20,24]. All known typical catalases exhibit discrete electronic spectrum with a strong absorbance in the Soret band (406–407 nm) and Rz (Reinheitszahl) values, indicating heme content of enzyme, were calculated around 1 (*i.e.* ratio of A_{Soret} nm/A_{280} nm) [42].

Phylogenetic analyses have revealed that monofunctional catalases fall into three distinct clades. Clade 1 catalases contain predominantly the plant enzymes, one algal example and one branch of bacterial catalases. Clade 2 enzymes are composed of only large subunit catalases with bacterial and fungal origins [5,14,29]. Clade 3 catalases contain only small subunit enzymes with bacterial, archaebacterial, fungal, and animal origins. The absence of Clade 3 enzymes in older taxonomic groups suggests that they evolved much later as a consequence of gene duplication in bacteria that then spread by horizontal and lateral transfers among bacteria to archaebacteria and eukaryotes [5,29].

The three-dimensional structures of 15 monofunctional heme catalases belonging to Clade 1, 2 and 3 have been determined at high resolution. The structures indicate that the heme group is deeply buried in

* Corresponding author.
E-mail address: yonca.yuzugullu@kocaeli.edu.tr (Y. Yuzugullu Karakus).

https://doi.org/10.1016/j.bbapap.2021.140662
Received 18 January 2021; Received in revised form 14 April 2021; Accepted 16 April 2021
Available online 19 April 2021
1570-9639/

Table 1
Oligonucleotides used in site-directed mutagenesis of *catpo*.

Mutant	Sequence change	Oligonucleotide*
V228A	GTT → GCT	5′-GCACATGGACGGCTTCGGTGCTCACACTTTCCGTTTC
V228C	GTT → TGC	5′-GCACATGGACGGCTTCGGTTGCCACACTTTCCGTTTC
V228F	GTT → TTC	5′-GCACATGGACGGCTTCGGTTTCCACACTTTCCGTTTC
V228G	GTT → GGT	5′-GCACATGGACGGCTTCGGTGGTCACACTTTCCGTTTC
V228I	GTT → ATC	5′-GCACATGGACGGCTTCGGTATCCACACTTTCCGTTTC
V228S	GTT → AGC	5′-GCACATGGACGGCTTCGGTAGCCACACTTTCCGTTTC

the core structure and its distance from the nearest part of the molecular surface is about 20 Å. The prosthetic group "heme" is linked to the molecular exterior by three channels: the main, the lateral and the central channels [9]. The main channel accesses the heme from above, while the lateral channel goes from the region of the NADP(H)-binding pocket in catalases that bind a nicotinamide cofactor to the proximal side of the heme. Contrarily, the central channel leads from the distal side of the heme to the central cavity of the enzyme [9]. The main channel is known to play a major role in catalytic activity, but the lateral channel has also recently been shown to also take part in catalytic activity [31].

S. thermophilum (Syn. *Mycothermus thermophilus/Humicola insolens*) is the dominant organism of mushroom compost and plays an important role in the production of the edible mushroom *Agaricus bisporus* [33,38]. Upon sporulation, *S. thermophilum* turns into a dark color due to extensive melanin formation [28]. This fungus is of industrial significance due to its ability to thrive on lignocellulosic compounds and the associated thermostable enzymes [13,30,43]. This industrially important fungus was previously reported to belong to Leotiomycetes but then has been reclassified in the Sordariales belong exclusively to the Chaetomiaceae and renamed as *Mycothermus thermophilus*, a thermophilic ascomycete with optimum growth temperatures between 45 and 50 °C [2].

We have previously shown that *S. thermophilum* secretes extracellular catalase enzyme which is a tetrameric protein containing a heme *d* in each active site. Amino acid sequence analysis and its three-dimensional structure analysis showed that the *Scytalidium* catalase belongs to monofuntional catalase family having large subunits. Besides the main peroxide degrading activity, the enzyme is also able to oxidize *o*-diphenolic and some *p*-diphenolic compounds in the absence of peroxide. Regarding its dual activity, the enzyme is then named as catalase-phenol oxidase (CATPO) [34,41]. We have observed that there is a binding pocket for oxidase substrates at the entrance to the lateral channel, in a pocket occupied by the nicotinamide moiety of NADPH in mammalian catalases [40]. We have also shown that replacing Val536 at the end of the lateral channel by Trp resulted in a very fast catalytic turnover rate but a 2.5-fold decrease in oxidase activity.

To further investigate the lateral channel, we have concentrated on an amino acid located close its start, adjacent to the heme. In the majority of catalases (62%), including CATPO, this is a valine. However, different residues such as serine (32%), glycine (%3), isoleucine (2%) and alanine (1%) are also found in other catalases [15] (Supplementary Fig. S1). A serine at this position has been shown to be crucial for electron transfer between NADPH and the heme in small subunit catalases [32]. Ile at same location is thought to hinder access to the lateral channel and this has been proposed as a cause of the slower turnover rates observed in some large subunit catalases [15].

To investigate the role of this position on catalytic activity in terms of both catalase and oxidase activities, 6 mutant variants of CATPO at position 228 were created, biochemically characterized and the crystallographic structures of two, V228C and V228I, determined at 1.47 and 1.41 Å resolution, respectively.

2. Experiments

2.1. Construction, purification and expression of Val228 variants

Chemicals and biochemicals used in experiments were purchased from Merck and Sigma. The oligonucleotides to create the desired variants, Val228Ala, Val228Cys, Val228Phe, Val228Gly, Val228Ile, and Val228Ser were designed and obtained from Sentegen, Turkey (Table 1).

Site-directed mutagenesis studies were performed using the QuikChange approach (Agilent) to alter the pET28TEV-CATPO plasmid [41]. Following confirmation of the mutated sequences, cloning and expression of variants were carried out using strains XL-1 Blue (Stratagene) and BL21 (DE3) Star (Invitrogen) of *Escherichia coli* respectively. The modified proteins were purified as described previously [41].

2.2. Activity assays of enzyme

Assays for catalase and phenol oxidase activities were carried out using the protocol described previously [40,41]. One unit of catalase is defined as the amount required to break down one micromole of H_2O_2 in one minute. Initial rates of H_2O_2 decomposition were used to estimate the turnover rate (k_{cat}) and the apparent K_M. Kinetic constants were obtained by fitting data to the Michaelis-Menten equation using Sigmaplot 14.0 (Systat Software Inc.). The term "K_{M_app}" [apparent K_M] in regard to catalases is defined as the substrate concentration at $V_{max}/2$. It is used here due to the fact that enzyme saturation is never achieved in the presence of excess substrate, hence the enzyme does not completely follow Michaelis-Menten kinetics [35]. One unit of phenol oxidase activity is described as the formation of one nanomole of product per minute. Protein concentration was calculated using the method defined by Bradford [3]. Assays were carried out in triplicate using an Agilent Cary 60 spectrophotometer.

2.3. UV–visible spectral analysis

All spectroscopic measurements were performed using an Agilent Cary 60 UV–Vis spectrophotometer at room temperature in a 1 cm quartz cuvette between 250 and 750 nm. The spectra were obtained with 0.5 mg ml^{-1} catalase in 20 mM sodium phosphate pH 7.4 at room temperature.

2.4. Crystallization and determination of structures

Hanging drop vapor diffusion method was used to obtain the crystals of the Val228 variants. The reservoir solution was composed of 6–16% (*v*/v) *polyethylene glycol 400,* 200 mM KCl, 10 mM $CaCl_2$, 50 mM sodium cacodylate in the pH values ranges from 5.0 to 5.6. 20% (v/v) *polyethylene glycol 400 was used as a* cryoprotectant *before* flash-cooling of crystals in liquid nitrogen [36]. Diffraction data were collected on

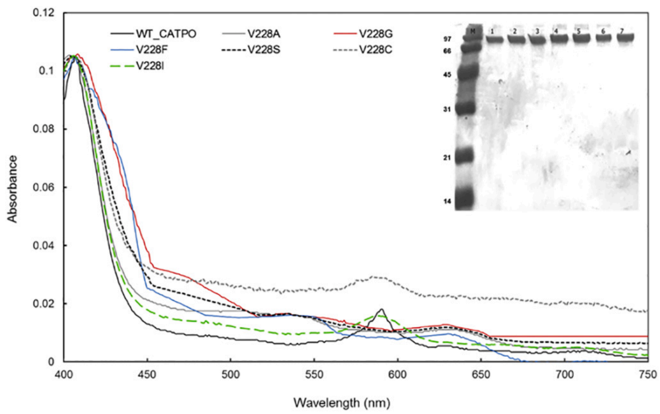

Fig. 1. Visible spectra of the CATPO and the V228A, V228C, V228F, V228G, V228I and V228S variants. The spectra were obtained with 0.5 mg ml^{-1} catalase in 20 mM sodium phosphate pH 7.4 at room temperature. The wild-type CATPO (WT_CATPO) spectrum is adjusted to have an equivalent value at the Soret peak for each of mutants. Insets, Coomassie-stained SDS–PAGE gels showing the purity of the CATPO variants. Lanes: M, molecular-mass marker; 1, WT_CATPO; 2, V228A; 3, V228C; 4, V228F; 5, V228G and 6, V228S (labelled in kDa). Full spectra are provided in Supplementary Fig. S2.

Beamline ID29 at European Synchrotron Radiation Facility (ESRF; [7,25]) at 100 K. Data were collected from a single crystal, each diffraction image was collected over a time period of 0.02 s and an oscillation range of 0.05 degrees. Processing, scaling, model building and refinement of diffraction data were carried out using XDS, Coot, REFMAC5 and other tools in the CCP4 suite [10,16,27,39], using the wild-type CATPO structure as a starting model (PDB: 4aum, [41]). The final structures of two variants out of seven on the lateral channel, V228C and V228I were resolved at 1.47 and 1.41 Å, respectively. Their structures of V228C and V228I variants have been deposited to the Protein Data Bank with accession codes of 5xzn and 5xzm, respectively. PyMOL was used for generating images (http://www.pymol.org/).

3. Results and discussion

We have previously shown that there is a substrate binding pocket for oxidase substrates at the entrance of the lateral channel, corresponding to the site of NADPH binding in mammalian catalases [40]. Val228 is situated adjacent to the heme edge at the entrance to this channel. It is moderately conserved in the majority of the catalases (about 62%) [15]. In order to investigate the role of Val228 on both oxidase and catalase activities, this residue was substituted with its equivalents in other catalases including Ala, Gly, Ile, Cys and Ser and Phe.

The catalase heme is either in the *d* or *b* form in monofunctional catalases and is found in one of two orientations that are “flipped” along the vinyl-propionate axis relative to one another [15]. In native CATPO, heme *d* has been identified by both crystallographic and spectroscopic analysis [41]. Among the CATPO variants tested here, V228C and V228I were observed to contain heme *d* by its characteristic 590 and 715 nm bands [22] in the absorbance spectra (Fig. 1). The presence of heme *d* was also confirmed by crystallographic analysis. The V228A, V228G, V228F and V228S variants contained heme *b* according to the UV–Vis spectral analysis (Fig. 1). Considering the characteristic absorption ratios for heme *d* (for recombinant wild type CATPO and the V228C and V228I variants) and heme *b* (for the V228A, V228G, V228F and V228S variants) from Table 3, they were consistent with those obtained for *E. coli* HPII wild type and its variants (for heme *d* containing variants: A590/A407 = 0.17–0.19 and A715/A407 = 0.04–0.06; for heme *b* containing variants A535/A407 = 0.11–0.14 and A630/A407 = 0.07–0.09) [22].

All monofunctional catalases are proposed to bind heme *b* at first; but later heme *d* is generated by cis-hydroxylation of heme *b* in a reaction catalyzed by large subunit catalase itself using hydrogen peroxide as a substrate [22]. Although large subunit catalases possessing either Val or Ile, near the edge of heme at the entrance of lateral channel contain heme *d* in their active site, small subunit catalases having Gly or Ser generally contain heme *b* (Supplementary Table S1). On the other hand, in HPII enzyme (large subunit enzyme), it has been shown that when I274 at the same location was converted to Ala, Val, Gly, and Cys all variants presented heme heterogeneity in the absorbance spectra, indicating a definite effect of the residue on heme packaging [15]. In our study, the V228A, V228G and V228S variants are found to have heme *b* in their active sites, while the V228I variant exhibited the presence of heme *d* in their structure. The presence of heme *b* in those variants can be explained in terms of less efficient retainment of substrate hydrogen peroxide in the heme cavity arising from easier escape through the more open entrance to the lateral channel; therefore, heme oxidation did not occur. Conversely, the bulky valine and isoleucine limit the peroxide movement and prevent it from escaping through lateral channel, and the longer occupancy in the cavity increases its chances of participating in oxidation reaction of heme *b* to heme *d* [15,22].

The A_{407}/A_{280} ratio or R_Z determines the protein purity and the amount of heme content. For wild type CATPO, the purified enzyme presents an R_Z value of *ca.* 0.8, but the R_Z values exhibited by V228A, V228G, V228F and V228S were much lower in the range of 0.2–0.3. The R_z values of V228C and V228I were also reduced compared to the wild type enzyme although not as much as other variants (Table 3). The low Rz values can be explained by either protein impurity or low heme content. Since the proteins are expressed well and purified with the >95% purity, we assume that the variants presented extremely low heme content. There is evidence in the literature to support the observation of an iron deficient catalase that still folds as long as the porphyrin ring is present, even though the iron itself is missing [1].

The kinetic parameters of the V228F and V228S variants indicated reduced catalase turnover rates (k_{cat}) but a similar affinity for peroxide to wild type. On the other hand, V228A, V228C, V228G and V228I variants exhibited increased turnover rates and higher $K_{M\text{-}app}$ values (lower affinities for substrate peroxide) than the wild type enzyme (Table 4).

According to a previous study in *E. coli* HPII catalase [31] it was proposed that widening the lateral channel caused an increase in the catalase activity. However, the opposite was also observed and catalytic efficiency was reduced in response to the enlargement of the channel diameter [15]. This is thought to be because the heme active site in each catalase clade has evolved to prolong the stay of H_2O_2 in the active center and opening the channel inlet may allow H_2O_2 to escape the active site before catalysis can occur. Our results demonstrate this is also true for Val 228 in CATPO. A reduction in catalase efficiency is observed when it is converted to any corresponding residue found in other cata-

Table 2
Crystallographic data-collection and refinement statistics. Values in parentheses are for the outermost shell.

	V228C variant	V228I variant
PDB code	5xzn	5xzm
Beamline	ID29, ESRF	ID29, ESRF
Detector	PILATUS 6 M-F	PILATUS 6 M-F
Transmission (%)	3.4	3.9
Wavelength (Å)	0.97	0.97
Space group	*I*2	*I*2
Unit-cell parameters		
a (Å)	125.1	125.5
b (Å)	121.1	120.3
c (Å)	185.11	183.7
β (°)	102.0	102.0
Resolution (Å)	112.84–1.45 (1.47–1.45)	112.84–1.41 (1.43–1.41)
R_{merge}[†] (%)	9.0 (61.0)	7.3 (80.0)
$R_{p.i.m.}$[‡] (%)	8.5 (56.6)	6.8 (73.2)
$CC_{1/2}$	0.992 (0.658)	0.997 (0.732)
# Observed reflections	430,890 (31778)	480,576 (34925)
# Unique reflections	22,662 (1711)	25,280 (1852)
Completeness (%)	99.2 (95.9)	99.2 (96.9)
Multiplicity	3.4 (3.4)	3.4 (3.4)
$\langle I/\sigma(I)\rangle$	7.4 (1.6)	8.6 (1.5)
Refinement		
R_{work} (%)	14.7 (25.3)	15.8 (29.9)
R_{free}[§] (%)	17.6 (27.4)	18.3 (30.7)
# protein atoms	22,639	21,905
# solvent molecules	2489	2113
# ligand atoms	352	256
# ion atoms	10	11
Average B factor (Å^2)		
Protein	14.9	15.0
Ligands	28.5	22.7
Solvent	19.1	19.3
Ions	15.1	18.3
R.m.s.d., bond lengths[¶] (Å)	0.022	0.022
R.m.s.d., bond angles[¶]	2.218	2.169
Ramachandran plot [††]		
Most favored regions (%)	96.96	97.58
Outliers (%)	0.11	0
Alignment with wild-type structure[‡‡] (PDB entry 4aum; [41]) over all residues		
R.m.s.d. (Å)	0.262	0.177
Q-score	0.980	0.992

† $R_{merge} = \sum_{hkl}\sum_i | I_i(hkl) — \{I(hkl)\} | \sum_{hkl}\sum_i | I_i(hkl)$.
‡ $R_{p.i.m.}$ is the precision-indicating (multiplicity-weighted) R_{merge}.
§ R_{free} was calculated with 5% of the reflections that were set aside randomly.
¶ Based on the ideal geometry values of Engh and Huber [11].
†† Ramachandran analysis using MolProbity [6].
‡‡ R.m.s.d and Q-scores were calculated using GESAMT [21].

lase clades.

We also examined the oxidase activities. The catechol oxidase activities of the V228I and V228F variants were remarkably reduced (42–59%) compared to wild-type CATPO, while the V228C variant had slight effect on the oxidase activity. Interestingly, the V228A, V228G and V228S variants exhibited high oxidase activities with a 402%, 580% and 254% increase with respect to the wild type enzyme (Table 4). In summary, conversion of Val228 to amino acids with larger side chains decreased oxidase activity, while the changes to hydrophobic/hydrophilic amino acids with smaller side chains considerably increased the oxidase activity. Our previous work has identified a putative oxidase substrate binding pocket at the end of the lateral channel, and we proposed that the oxidase activity was as a result of electron transfer to the heme, rather than direct interaction of the oxidase substrate with a high valent iron-oxo species at the heme [40]. The increase in oxidase activity upon mutation of Val228 to a small residue could result in an alteration of the water structure in the lateral channel that facilitates this electron transfer. An alternative hypothesis is that the lateral channel is "opened", allowing the oxidase substrate to approach more closely to the heme. To explore this further we attempted to crystallize the Val228 variants.

Table 3
Spectroscopic characterization of CATPO variant heme content.

Variant	Rz (A_{407}/A_{280})	A_{590}/A_{407}	A_{715}/A_{407}	A_{535}/A_{407}	A_{630}/A_{407}
WT	0.8	0.17	0.03	–	–
V228A	0.3	–	–	0.16	0.1
V228C	0.6	0.27	0.19	–	–
V228F	0.3	–	–	0.15	0.09
V228G	0.2	–	–	0.16	0.1
V228I	0.6	0.15	0.04	–	–
V228S	0.2	–	–	0.16	0.1

The crystal structures of two variants, V228C (low catalase activity and little effect on oxidase activity) and V228I (similar catalase activity to wild type and little effect on oxidase activity), were determined at 1.47 and 1.41 Å, respectively. Despite comprehensive trials, V228A and V228G crystals remain elusive (highest oxidase activities). Crystals of V228C and V228I show the same overall structure as the wild-type CATPO but are in an alternative space group, I2, compared to the wild-type CATPO (PDB: 4aum, [41]) which crystallizes in the space

Table 4
Kinetic constants.

Variant	K_{M_app}† (m*M*)	k_{cat} (s^{-1})	k_{cat}/K_{M_app} (s^{-1} M^{-1})	R_Z‡	Heme type	Specific catalase activity (μmole mg^{-1} min^{-1})	Specific oxidase activity (nmole mg^{-1} min^{-1})
CATPO	10	20.3×10^4	20.3 X 10^3	0.8	*d*	18,713 ± 935	213 ± 5
V228A	249	31.3×10^4	1.3 X 10^3	0.3	*b*	3781 ± 248	856 ± 69
V228C	400	83.2×10^4	2.1 X 10^3	0.6	*d*	6408 ± 81	269 ± 27
V228F	17	4.5×10^4	2.7 X 10^3	0.3	*b*	125 ± 23	88 ± 18
V228G	180	41.1×10^4	2.3 X 10^3	0.2	*b*	1464 ± 48	1236 ± 196
V228I	300	150.0×10^4	5.0 X 10^3	0.6	*d*	18,559 ± 540	123 ± 20
V228S	18	12.0×10^4	7.0 X 10^3	0.2	*b*	20 ± 6	540 ± 35

† K_{M_app} is the H_2O_2 concentration at $V_{max}/2$ and is used because the catalase reaction does not saturate with substrate and therefore does not precisely follow Michaelis–Menten kinetics [35].

‡ $R_Z = A_{407}/A_{280}$. The values were normalized to heme content in each CATPO variant, a full table with normalized and unnormalized values is provided as supplementary data. Heme type was determined according to the presence of diagnostic absorbance bands at 590 nm (heme *d*) or 630 nm (heme *b*).

group C2. Electron density maps confirm the d type heme for both variants. Both variants show a high Q-scores with low Root Mean Square Deviation values (Table 2) indicating that V228C and V228I are almost identical with wild-type CATPO.

The expected side chains at position 228 were evident for V228C, and V228I (Fig. 2). Surprisingly, no covalent linkage was observed in the V228C, although Cys-heme crosslink in the equivalent residue to V228 in catalase HPII (I274) from *E. coli* was previously reported [15] (Supplementary Table S1).

In the active site cavity, the feature common to both variants is the absence of water 3 (W3), whereas nearby water 2 (W2) is present in the active sites of all variants (Fig. 3). Another common feature is that both structures lacked water 8 (W8) located in the upper main channel. In V228C, water 7 (W7) is also missing which was consistent with partial decrease in catalytic activity. In the lateral channel, an almost identical chain of ordered waters was detected in V228C and V228I variants to that observed for wild-type (Fig. 3). This was also in agreement with similar oxidase activity values measured in these variants to that for wild type CATPO (Table 4). For the V228A, V228G and V228S variants with higher oxidase activities than wild type, we assume that this increase could be due to an improved electron transfer to the heme, or a closer access of the oxidase substrate to the heme. To distinguish these possibilities a structure of the variants in complex with either an oxidase substrate or inhibitor would be very useful, however to date we have been unable to obtain such a species, either by co-crystallization or soaking.

4. Conclusion

Our study reports on the role of Val228 in *Scytalidium* catalase based on kinetic data of the variants as well as the structural characterizations of two variants. A change of valine to almost all amino acid residues tested including alanine, glycine, cysteine, phenylalanine and serine (except isoleucine) resulted in a significant reduction in catalase activity and a lower heme content. On the other hand, introduction of smaller side chains at this position markedly increased the oxidase activity. These results indicate that Val228 has an important role in both heme incorporation and on both catalase and oxidase activity, explaining why this residue is semi-conserved in catalases.

Author contributions

GG & SB generated the mutants and expressed all the proteins. GG crystallized the proteins and carried out the kinetic studies. GG, BAY, & ARP collected and processed X-ray diffraction data and refined the structures. YYK & ARP conceived the project, and guided the work. GG & YYK wrote the paper. All authors contributed to discussion of the results and experiment design and have approved the final version of the manuscript.

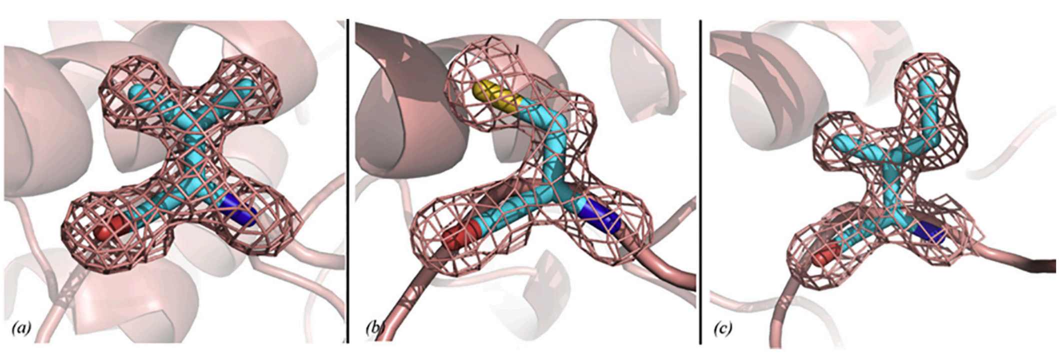

Fig. 2. 2Fo-Fc Electron density maps (shown in pink) of Val228 (a), Cys228 (b) and Ile228 (c) at 1.0 r.m.s.d.

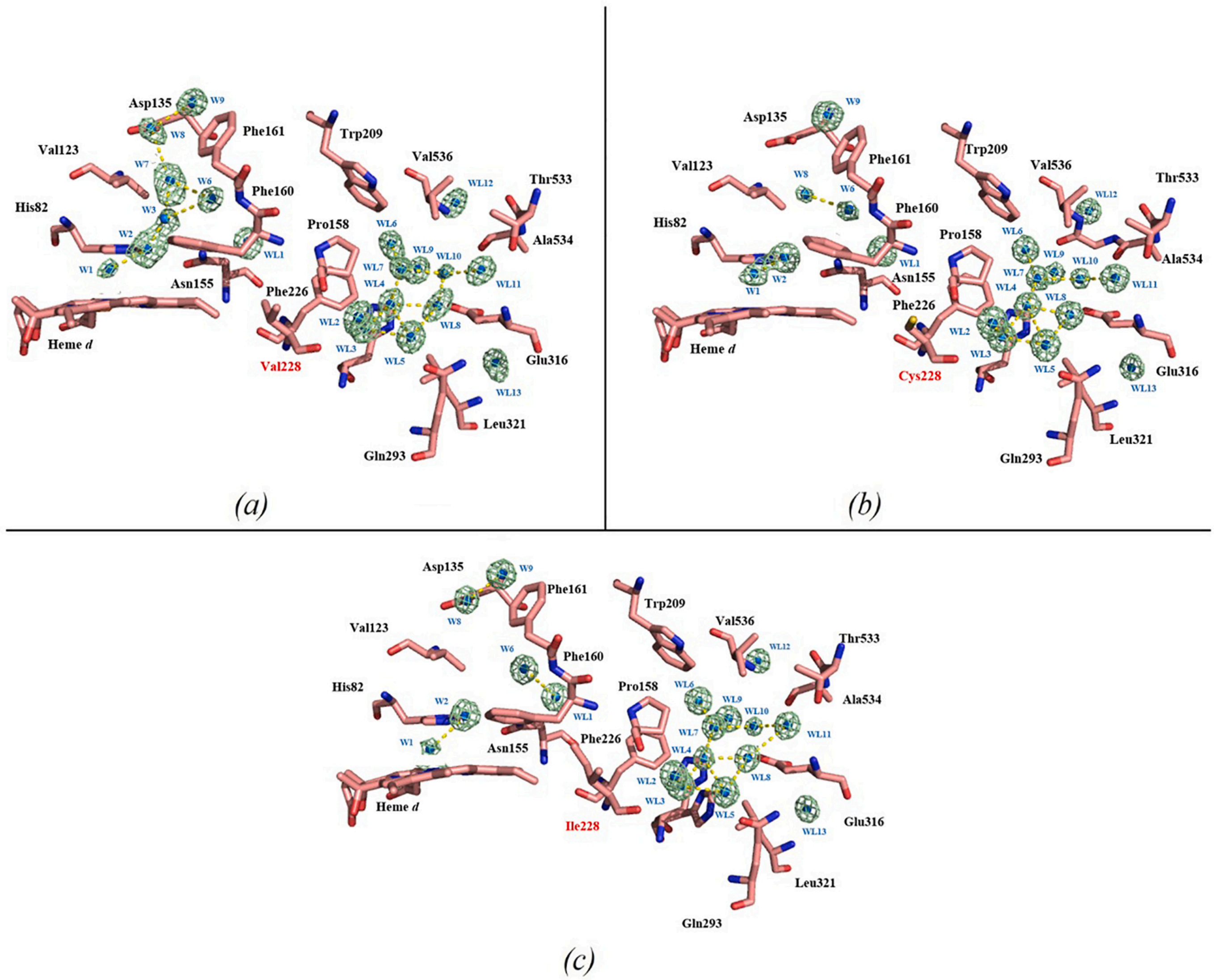

Fig. 3. Comparison of main and lateral channel waters for wild type CATPO (a), V228C (b) and V228I (c). Mutations are shown in red, electron density maps for water molecules illustrated at 0.8 r.m.s.d as green mesh. Waters in the lateral channel are labelled as WLX and in the main channel as WX, where X is the water number. The electron density maps for the residues along with water molecules are provided in Supplementary Figs. S3–S5.

Funding sources

This work was made possible by generous support from the EU COST Action CM1306 "Movement and Mechanism in Molecular Machines". YYK, GG and SB would like to thank TÜBİTAK (Grant Number: 113Z744) for funding. ARP is supported by the German Federal Excellence Cluster "Hamburg Centre for Ultrafast Imaging" (EXC1074). BAY is supported by a Henry Wellcome Fellowship (Wellcome Trust 110296/Z/15/Z).

Notes

The authors declare no competing financial interests.

Declaration of Competing Interest

The authors declare that they have no known competing financial interests or personal relationships that could have appeared to influence the work reported in this paper.

Appendix A. Supplementary data

Supplementary data to this article can be found online at https://doi.org/10.1016/j.bbapap.2021.140662.

References

[1] P. Andreoletti, G. Sainz, M. Jaquinod, J. Gagnon, H.M. Jouve, Proteins Struct. Funct. Genet. 50 (2003) 261–271, https://doi.org/10.1002/prot.10283.
[2] N. Basotra, B. Kaur, M. Di Falco, A. Tsang, B.S. Chadha, Bioresour. Technol. 222 (2016) 413–421, https://doi.org/10.1016/j.biortech.2016.10.018.
[3] M.M. Bradford, Anal. Biochem. 72 (1976) 248–254, https://doi.org/10.1016/0003-2697(76)90527-3.
[4] J. Bravo, I. Fita, J.C. Ferrer, W. Ens, A. Hillar, J. Switala, P.C. Loewen, Protein Sci. 6 (1997) 1016–1023.
[5] P. Chelikani, I. Fita, P.C. Loewen, Cell. Mol. Life Sci. 61 (2004) 192–208, https://doi.org/10.1007/s00018-003-3206-5.
[6] V.B. Chen, W.B. Arendall, J.J. Headd, D.A. Keedy, R.M. Immormino, G.J. Kapral, L. W. Murray, J.S. Richardson, D.C. Richardson, Acta Cryst D66 (2010) 12–21.
[7] D. de Sanctis, et al., J. Synchrotron Rad. 19 (2012) 455–461, https://doi.org/10.1107/S0909049512009715.
[8] A. Díaz, R.A. Muñoz-Clares, P. Rangel, V.J. Valdés, W. Hansberg, Biochimie 87 (2005) 205–214, https://doi.org/10.1016/j.biochi.2004.10.014.
[9] A. Díaz, P.C. Loewen, I. Fita, X. Carpena, Arch. Biochem. Biophys. 525 (2012) 102–110, https://doi.org/10.1016/j.abb.2011.12.011.

[10] P. Emsley, B. Lohkamp, W.G. Scott, K. Cowtan, Acta Cryst D66 (2010) 486–501, https://doi.org/10.1107/S0907444910007493.
[11] R.A. Engh, R. Huber, Acta Cryst A47 (1991) 392–400, https://doi.org/10.1107/S0108767391001071.
[12] J.A. Frugoli, M.A. McPeek, T.L. Thomas, C.R. McClung, Plant Physiol. 112 (1998) 327–336, https://doi.org/10.1104/pp.112.1.327.
[13] L.H. Guimarães, H.F. Terenzi, J.A. Jorge, M.L. Polizeli, J. Ind. Microbiol. Biotechnol. 27 (2001) 265–270, https://doi.org/10.1038/sj.jim.7000196.
[14] I. Hara, N. Ichise, K. Kojima, H. Kondo, S. Ohgiya, H. Matsuyama, I. Yumoto, Biochemistry 46 (2007) 11–22, https://doi.org/10.1021/bi061519w.
[15] V. Jha, S. Louis, P. Chelikani, Biochem. 50 (2011) 2101–2110, https://doi.org/10.1021/bi200027v.
[16] W. Kabsch, Acta Cryst D66 (2010) 125–132, https://doi.org/10.1107/S0907444909047337.
[17] K. Karlin, Science 261 (1993) 701–708, https://doi.org/10.1126/science.7688141.
[18] J.A. Kim, Z. Sha, J.E. Mayfield, Infect. Immun. 68 (2000) 3861–3866, https://doi.org/10.1128/IAI.68.7.3861-3866.2000.
[19] M.G. Klotz, P.C. Loewen, Mol. Biol. Evol. 20 (2003) 1098–1112, https://doi.org/10.1093/molbev/msg129.
[20] M. Klotz, G. Klassen, P.C. Loewen, Mol. Biol. Evol. 14 (1997) 951–958, https://doi.org/10.1093/oxfordjournals.molbev.a025838.
[21] E. Krissinel, J. Mol. Biochem. 1 (2012) 76–85.
[22] P.C. Loewen, J. Switala, I. von Ossowski, A. Hillar, A. Christie, B. Tattrie, P. Nicholls, Biochem. 32 (1993) 10159–10164.
[23] M.J. Maté, G. Murshudov, J. Bravo, W. Melik-Adamyan, P.C. Loewen, I. Fita, in: R. A. Scott (Ed.), Encyclopedia of Inorganic and Bioinorganic Chemistry, John Wiley & Sons, New York, 2001, pp. 486–502.
[24] J.E. Mayfield, M.R. Duvall, J. Mol. Evol. 42 (1996) 469–471, https://doi.org/10.1007/BF02498641.
[25] A.A. McCarthy, et al., J. Synchrotron Radiat. 25 (2018) 1249–1260, https://doi.org/10.1107/S1600577518007166.
[26] S. Mueller, H.D. Riedel, W. Stremmel, Anal. Biochem. 245 (1997) 55–60, https://doi.org/10.1006/abio.1996.9939.
[27] G.N. Murshudov, P. Skubák, A.A. Lebedev, N.S. Pannu, R.A. Steiner, R.A. Nicholls, M.D. Winn, F. Long, A.A. Vagin, Acta Cryst D67 (2011) 355–367, https://doi.org/10.1107/S0907444911001314.
[28] D.O. Natvig, J.W. Taylor, A. Tsang, M.I. Hutchinson, A.J. Powell, Mycologia 107 (2015) 319–327, https://doi.org/10.3852/13-399.
[29] P. Nicholls, I. Fita, P.C. Loewen, Adv. Inorg. Chem. 51 (2001) 51–106.
[30] Z.B. Ögel, K. Yarangümeli, H. Dü, I. Ifrij, Enzym. Microb. Technol. 28 (2001) 689–695, https://doi.org/10.1016/s0141-0229(01)00315-5.
[31] M.S. Sevinc, M.J. Maté, J. Switala, I. Fita, P.C. Loewen, Protein Sci. 8 (1999) 490–498, https://doi.org/10.1110/ps.8.3.490.
[32] W. Sicking, H.-G. Korth, H. de Groot, R. Sustmann, J. Am. Chem. Soc. 130 (2008) 7345–7356, https://doi.org/10.1021/ja077787e.
[33] G. Straatsma, R.A. Samson, T.W. Olijnsma, H.J. Op Den Camp, J.P. Gerrits, L.J. Van Griensven, Appl. Environ. Microbiol. 60 (1994) 454–458, https://doi.org/10.1128/AEM.60.2.454-458.1994.
[34] D. Sutay Kocabas, U. Bakir, S.E.V. Phillips, M.J. McPherson, Z.B. Ogel, Appl. Microbiol. Biotechnol. 79 (2008) 407–415, https://doi.org/10.1007/s00253-008-1437-y.
[35] J. Switala, P.C. Loewen, Arch. Biochem. Biophys. 401 (2002) 145–154, https://doi.org/10.1016/S0003-9861(02)00049-8.
[36] T.-Y. Teng, J. Appl. Crystallogr. 23 (1990) 387–391, https://doi.org/10.1107/S0021889890005568.
[38] W.M. Wiegant, J. Wery, E.T. Buitenhuis, J.A. de Bont, Appl. Environ. Microbiol. 58 (1992) 2654–2659, https://doi.org/10.1128/AEM.58.8.2654-2659.1992.
[39] M.D. Winn, C.C. Ballard, K.D. Cowtan, E.J. Dodson, P. Emsley, P.R. Evans, K. S. Wilson, Acta Cryst D67 (2011) 235–242, https://doi.org/10.1107/S0907444910045749.
[40] Y. Yuzugullu Karakus, G. Goc, S. Balci, B.B. Yorke, C.H. Trinh, M.J. McPherson, Acta Cryst D74 (2018) 979–985, https://doi.org/10.1107/S2059798318010628.
[41] Y. Yuzugullu, C.H. Trinh, M.A. Smith, A.R. Pearson, S.E.V. Phillips, D. Sutay Kocabas, U. Bakir, Z.B. Ogel, M.J. McPherson, Acta Cryst D69 (2013) 398–408, https://doi.org/10.1107/S0907444912049001.
[42] M. Zámocký, F. Koller, Prog. Biophys. Mol. 72 (1999) 19–66, https://doi.org/10.1016/S0079-6107(98)00058-3.
[43] F.F. Zanoelo, L. Polizeli Mde, H.F. Terenzi, J.A. Jorge, FEMS Microbiol. Lett. 240 (2004) 137–143, https://doi.org/10.1016/j.femsle.2004.09.021.